# Measurements of Antenna Parameters in GTEM Cell

Zlatko Živković, Antonio Šarolić

***Abstract:*** **The paper presents the method for measuring parameters (gain, antenna factor, impedance and radiation pattern) of small antennas in GTEM cell, which is a novel method and environment for antenna measurements. In order to investigate the suitability of GTEM cell for this kind of measurement, the measurement results for a biconical dipole, microstrip patch antennas and small loop antenna were compared with those obtained by calibration inside fully absorber lined anechoic site, two-antenna measurements and FEKO simulations. The measurements were carried out over the wide frequency range. Measurement setup was limited to small antennas that fit into the usable test volume of the GTEM cell. Different sizes that satisfy this restriction were examined. The GTEM measurement results showed considerable agreement with compared results.**

***Index terms:*** **antenna measurements, GTEM cell, FEKO simulation, biconical antenna, microstrip patch antenna, small loop antenna**

## I. INTRODUCTION

The Gigahertz Transverse Electromagnetic (GTEM) cell is a test environment widely used for EMC susceptibility and emission measurements [1-3]. However, regarding well-defined polarization and homogeneity of electric and magnetic fields inside GTEM cell, it was also proposed for small antenna measurements [4-9], as a less expensive, but yet reliable measurement environment compared to anechoic chambers. The purpose of this paper is to examine and confirm the usability of GTEM cell for antenna measurements.

GTEM cell represents a tapered coaxial line terminated by a combination of resistors and RF absorbers, providing characteristic impedance of Z = 50 Ω over the wide frequency range. When a GTEM cell is excited by RF power at its input port, the TEM wave propagates along the septum, ensuring well-defined polarization of the electromagnetic wave. The field homogeneity is adequate as long as the dimensions of measured objects are within the limits of the test volume of GTEM. The generated electric field inside a GTEM cell is directly correlated to the input voltage (or power) [10].

In this paper, the measurement methods of small antenna parameters (antenna factor, gain, impedance and radiation pattern) in GTEM cell are described and the results are compared with those obtained by the measurements performed outside of the cell and FEKO simulations. In order to examine the behavior of different antennas in GTEM cell, the broadband biconical dipole [11], rectangular microstrip antenna (RMSA) and circular microstrip antenna (CMSA) [12] and small loop antenna [13] were used for this study. The gain of broadband biconical dipole and microstrip antennas were measured, while the small loop antenna was used to measure radiation pattern in GTEM cell. Additionally, the input impedance of microstrip patch antennas was measured inside and outside of GTEM cell. Thus, the measurements were performed over the wide frequency range (25.11 MHz – 3GHz) and antennas with different dimensions were used, provided that they fit into the usable test volume of the GTEM cell. However, due to scattering from device-under-test (DUT) and reflections from the cell discontinuities, significant deviation from theoretically predicted electric field strength can occur [14]. In order to observe this phenomenon, the electric field strength was controlled by an isotropic electric field probe and input power was adjusted as needed.

The antennas were mounted inside the GTEM cell and exposed to the incident electric field with known magnitude. The gain and radiation pattern were then calculated from the received power displayed by spectrum analyzer. The measurement setup for impedance was based on Vector Network Analyzer (VNA). By measuring magnitude and phase of reflection coefficient the input impedances of examined antennas were obtained. Each antenna was additionally modeled using FEKO software suite.

## II. ANTENNAS AND SIMULATION MODELS

### *A. Broadband biconical dipole*

As an example of small antenna, the commercially available broadband biconical dipole PCD 8250 with matching balun was used (Fig. 1a) [11]. The dipole was 7 cm wide and 13 cm high with half-cone angle $\alpha/2 = 25°$. In order to compare the results of measured gain and antenna factor, the biconical dipole without matching balun was modeled with FEKO simulation software (Fig. 1b) and the input impedance and gain were calculated. Concerning the dimensions, the antenna model in FEKO was identical to the real biconical dipole. The voltage source in FEKO simulation was positioned in the middle of short wire (5 mm) that connected two cones.

The FEKO model was meshed with over 2000 triangular segments (Fig. 1c). All mesh triangles satisfied segmentation rules, without errors or warnings reported during calculations.

Manuscript received October 20, 2010, revised November, 2010.

This research was supported by the Ministry of Science, Education and Sports of the Republic of Croatia (Projects No. 023-0000000-3237 and No. 036-0361630-1631).

Z. Živković and A. Šarolić are with University of Split, Split, Croatia. (email: {zlatko.zivkovic, antonio.sarolic}@fesb.hr}).

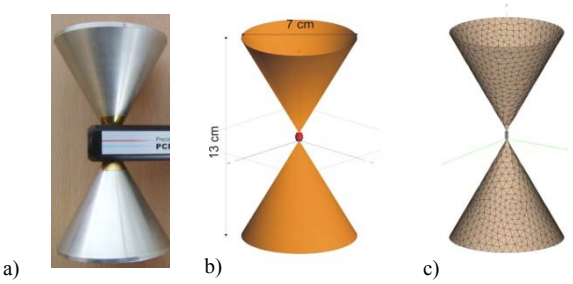


Fig.1. a) Real biconical antenna, b) Simulation model in FEKO, c) Meshed structure

### *B. Microstrip patch antennas*

The examined microstrip antennas were fabricated in antenna laboratory at University of Split, FESB [12]. The microstrip patch antennas were printed on the substrate having dielectric constant $\varepsilon_r = 2.3$ and thickness $h = 1.6$ mm. The conducting layers on both side of printed board were made of copper.

The dimensions of RMSA (Fig. 2a) at resonant frequency $f = 2.4$ GHz were obtained by procedures and equations described in [15], which yielded the width $W = 4.86$ cm, and length $L = 4.04$ cm. Both antennas were fed by coaxial feed. In order to obtain the input impedance of 50 Ω at the resonant frequency, the position of coaxial feed point was set at distance $x_R = 0.63$ cm from the centre of the patch.

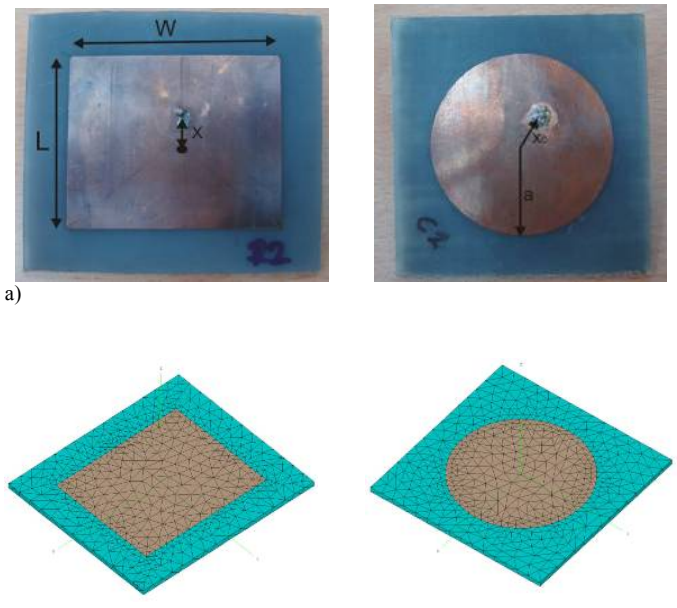


Fig. 2. Rectangular and circular microstrip antennas: a) real antennas, b) simulation models

The dimensions of CMSA (Fig. 2a) at the same resonant frequency were obtained by equations provided in [16]. The radius of a patch was set to $a = 2.41$ cm, and the coaxial feed was set at distance $x_C = 0.88$ cm from the patch centre.

The size of the ground plane was greater than the patch dimensions by approximately six times the substrate thickness [15]. Therefore overall dimensions of RMSA were $W_R = 6.86$ cm, $L_R = 6.04$ cm, and the overall dimensions of CMSA were $W_C = 6.81$ cm, $L_C = 6.81$ cm.

The simulation model was built according to [17]. The simulated antennas were identical to the real examined antennas regarding the dimensions of antennas and electrical parameters of printed board. The models were meshed with over 1000 triangle segments (Fig 2b). All segmentation rules were satisfied so there were no errors or warnings reported during the calculation.

### *C. Small loop antenna*

In order to measure antenna radiation pattern in GTEM cell, small loop antenna, described in [13] was created (Fig. 3a). This kind of loop antenna is used for RFID at 13.56 MHz. Its original dimensions were 50×50 cm, but due to dimension limitations of antennas that can be measured in our GTEM cell, whole antenna was scaled by factor 0.54. Thus, the final dimensions of antenna were 27×27 cm which is around the upper limit for the antenna dimensions that can be measured in our GTEM cell. As a consequence, the frequency was changed to 25.11 MHz, so the electrical dimensions of antenna remained unchanged. The loop was created of thin copper ribbons, 19 mm wide, fixed to the styrofoam substrate. The antenna was fed with coaxial cable.

The model of identical loop antenna was made in FEKO (Fig. 3b). It consisted of more than 2000 segmentation triangles for MoM calculation so there were no errors or warnings found during computation.

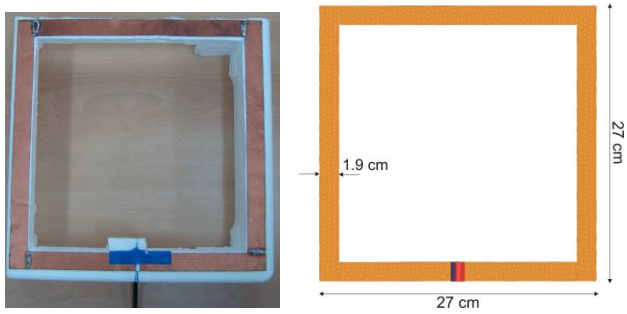


Fig. 3. Loop antenna: a) created loop antenna, b) simulation model

## III. MEASUREMENT SETUPS

### *A. Theoretical background*

Since the dominant mode in the GTEM cell is TEM mode the gain of antenna $G$ can be calculated from equation:

$$P_{rec} = S_i \cdot A_{ef} = \frac{E_i^2}{Z_0} \cdot \frac{\lambda^2}{4\pi} \cdot G \qquad (1)$$

where $P_{rec}$ is received power at the tested antenna for a given incident electric field $E_i$, $S_i$ is the incident power density, $A_{ef}$ is the effective antenna aperture, $Z_0 = 120\pi$ Ω is field wave impedance in GTEM cell and $\lambda$ is wavelength. Using well-known relation $c = \lambda \cdot f$, where $c$ is the speed of light, and $f$ is

signal frequency, and equation (1), the expression for gain can be obtained:

$$G = 525.84 \cdot 10^{-16} \cdot f^2 \cdot \frac{P_{rec}}{E_i^2}, \quad (2)$$

or in decibels:

$$G\ [\mathrm{dBi}] = -132.8 + 20 \log f + P_{rec}\,[\mathrm{dB}] - E_i\,[\mathrm{dBV/m}]. \quad (3)$$

Equations (2) and (3) define the necessary measurements for obtaining antenna gain at a certain frequency in GTEM cell. It can be shown that by measuring incident electric field and received power the antenna factor can be obtained as well.

The antenna factor is defined as:

$$AF = \frac{E_i}{V} = \frac{E_i}{\sqrt{P_{rec} \cdot Z_C}} = 0.141 \cdot \frac{E_i}{\sqrt{P_{rec}}}, \quad (4)$$

or in decibels:

$$AF\ [\mathrm{dBm^{-1}}] = -17 + E_i\,[\mathrm{dBV/m}] - P_{rec}\,[\mathrm{dB}], \quad (5)$$

where $V = \sqrt{P_{rec} \cdot Z_C}$ is the output voltage at the antenna terminals and $Z_C = 50\ \Omega$ is impedance of the antenna load (RF cables connected to the spectrum analyzer).

Regarding the fact that FEKO does not calculate the antenna factor, it was calculated manually using simulation results of antenna gain. By equalizing the expressions for received power (1) and (4) the following equation was obtained:

$$\frac{E^2}{Z_C \cdot AF^2} = \frac{E^2}{120\pi} \cdot \frac{\lambda^2}{4\pi} \cdot G \quad (6)$$

which yields the expression for antenna factor of simulated antenna:

$$AF^2 = 1.05 \cdot 10^{-15} \cdot \frac{f^2}{G} \quad (7)$$

or in decibels:

$$AF\left[\mathrm{dBm^{-1}}\right] = -149.7 + 20 \log f - G\,[\mathrm{dBi}]. \quad (8)$$

*B. Antenna gain and antenna factor measurement setup*

The measurement setups for antenna gain and antenna factor are depicted in Fig. 4. The measurements were performed in TESEQ 750 GTEM cell with maximum septum height of 750 mm. The PCD 8250 biconical antenna with broadband matching balun (Fig. 5a) was mounted vertically on styrofoam table in the centre of the test volume (center third of the septum height). Generic setup for GTEM measurements can be found in [2, 3]. The antenna axis was positioned in parallel with electric field vector, so there were no losses due to polarization mismatch. The antenna dimensions (cone diameter was 7 cm and overall height was 13 cm) were small enough compared to septum height, so the required demand for homogeneity of electric field was completely satisfied. The antenna was connected to Anritsu MS2663C spectrum analyzer via RG213 coaxial cable. The vertical part of cable was positioned behind the dipole (between RF absorbers) and the rest of it was laid down along the cell's floor (Fig. 4a). This kind of cable positioning ensured minimal electric field perturbation [5].

The measurements were performed over the entire operational frequency range of the PCD 8250 biconical antenna that was declared by manufacturer (80 MHz – 3 GHz). The frequency step of 54.8 MHz was chosen which yielded 51 frequency points in declared frequency band.

Measurement setup for the microstrip antennas was identical to the measurement setup for biconical dipole (Fig. 4). The position of patch antennas inside GTEM cell is shown at Fig. 5b. Regarding the fact that the resonant frequency of antennas was aimed to be 2.4 GHz, the measurements were performed over the frequency range from 2 GHz to 2.8 GHz. The frequency step of 50 MHz was chosen which yielded 17 frequency points in declared frequency band.

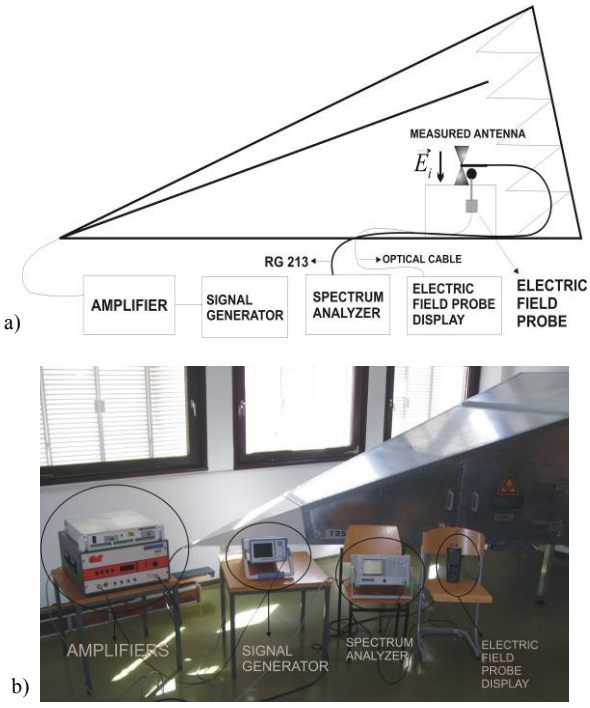


Fig. 4. Measurement setup for gain and antenna factor measurement of the biconical dipole and microstrip antennas: a) schematic view, b) instrumentation

The input CW signal was generated by Rohde & Schwarz SM300 signal generator via RF power amplifiers Ophir 5140 and AR 150W1000. The AR 150W1000 amplifier was used for frequencies below 750 MHz, and Ophir 5140 amplifier was used for higher frequencies up to 3 GHz. The electric field magnitude of 10 V/m (20 dBV/m) at the position of measurement was achieved, over the whole frequency range, by adjusting input signal power on signal generator. The wanted field magnitude was checked by isotropic electric field probe HI-4455 that was positioned next to biconical dipole

and microstrip antennas during the measurement procedure (Fig. 5). Field probe was connected with its display outside of cell via optical cable, so the field perturbation by its presence could be neglected.

The final expressions for gain and antenna factor are obtained from (3) and (5), setting the incident electric field strength to 20 dBV/m, and taking into account the cable loss ($L_{coax}$) from the received power at the antenna ($P_{rec}$) to the power displayed on spectrum analyzer ($P_{SA}$):

$$G\ [\mathrm{dBi}] = -152.8 + 20\log f + P_{SA}\,[\mathrm{dB}] + L_{coax}\,[\mathrm{dB}], \quad (9)$$

$$AF\ \left[\mathrm{dBm^{-1}}\right] = 3 - P_{SA}\,[\mathrm{dB}] - L_{coax}\,[\mathrm{dB}]. \quad (10)$$

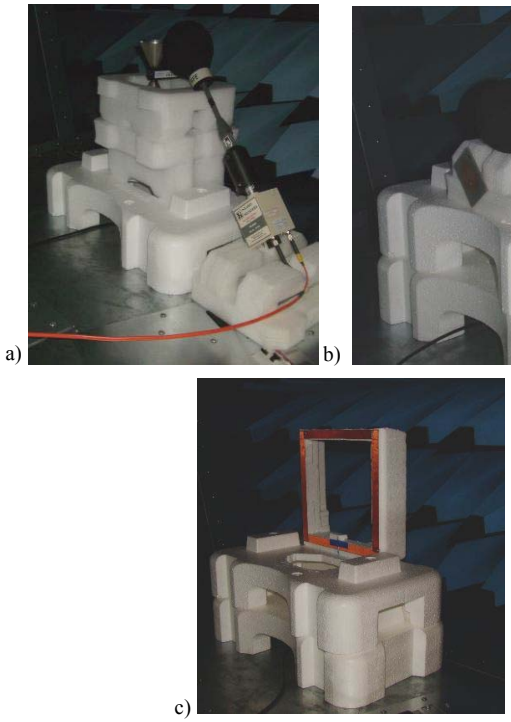

Fig. 5. Position of a) biconical dipole and b) microstrip antennas, with electric field probe inside the GTEM cell, c) loop antenna

*C. Antenna impedance measurement setup*

The antenna impedance measurement setup was based on VNA HP8720A that was connected to PC via HP-IB bus (Fig. 6). The input impedance of microstrip antennas was obtained by measuring the magnitude and phase of the reflection coefficient $S_{11}$. The impedance was then calculated using equation:

$$Z_{in} = Z_L \frac{1 + |S_{11}| e^{j\varphi}}{1 - |S_{11}| e^{j\varphi}} \quad (11)$$

where $Z_L$ = 50 Ω is the characteristic impedance of the coaxial cable and $\varphi$ is the phase of $S_{11}$.

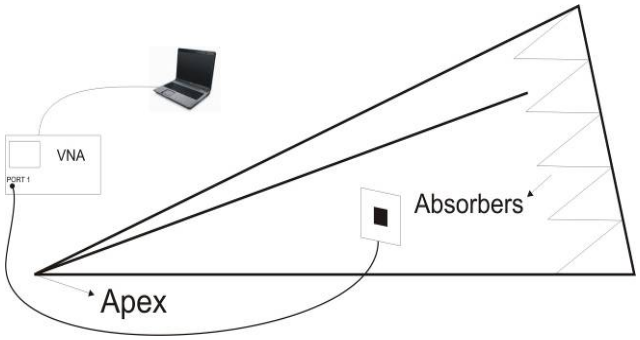


Fig. 6. Input impedance measurement setup

Two sets of measurements were performed in order to compare the results for different orientations of microstrip antennas in GTEM cell (Fig. 7). In the first set, the antennas were directed toward the RF absorbers, and in the second set, the antennas were directed toward the input/output (apex) of the cell. During all measurements, the input/output of the cell was terminated by 50 Ω broadband termination.

The measurements were performed over the frequency range from 2 GHz to 2.8 GHz. The frequency step of 2.5 MHz was chosen which yielded 321 frequency points in the declared frequency band.

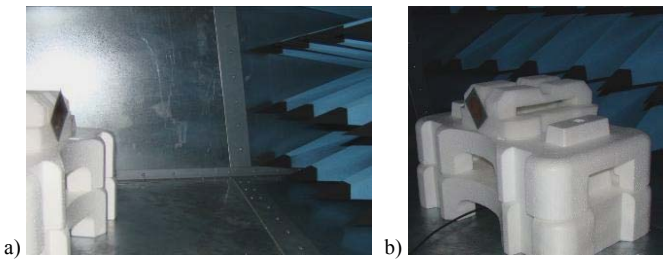

Fig. 7. Orientation of the antennas in GTEM cell: a) toward absorbers, b) toward input/output

For the purpose of results assessment, another measurement of antenna impedance was performed outside of the cell. The measurement environment was not completely free of reflective objects, but they were sufficiently far from the antennas to affect their impedance significantly.

*D. Radiation pattern measurement setup*

The measurement setup for radiation pattern of loop antenna was identical to the setup for antenna gain measurements. The constant electric field strength was controlled by isotropic electric field probe. The antenna was rotated around vertical axis in 10° steps, as it is presented in Fig. 8. The position of examined antenna in GTEM cell is shown in Fig. 5c. The radiation pattern measurements were carried out at frequency of 25.11 MHz.

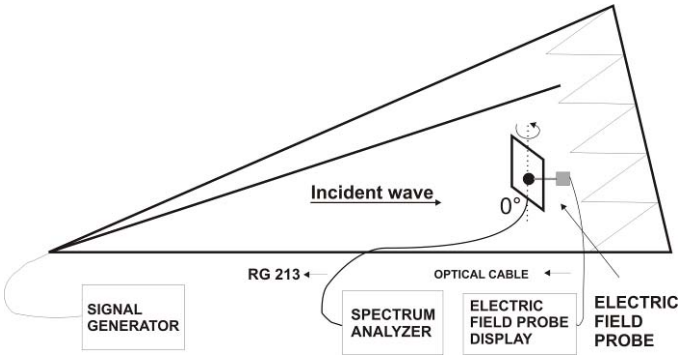


Fig 8. Measurement setup for radiation pattern

## IV. Measurement and Simulation Results

### *A. Results for antenna gain and antenna factor*

The measurement results for biconical dipole, altogether with calibration and simulation results are presented in Fig. 9a and Fig. 10a. Additionally, the input antenna impedance for biconical dipole without broadband matching balun is presented in Fig. 11. The measurements performed in GTEM cell showed good agreement with those obtained during calibration process in fully lined anechoic site at an accredited laboratory. The mean difference and standard deviation as compared to calibration results were $\bar{x} = -1$ dB and $\sigma$ = 1.9 dB respectively. However, the reason of this deviation was standard measurement uncertainty of spectrum analyzer and isotropic electric field probe, rather than the field perturbation in the GTEM cell, due to the fact that the incident field was continuously controlled. The combined standard uncertainty of two measuring instruments (spectrum analyzer and field probe) can be obtained by [18]:

$$u_{MS} = \sqrt{u_{SA}^2 + u_{FP}^2} = \sqrt{1.3^2 + 1^2} = 1.65 \text{ dB} \qquad (12)$$

where $u_{SA}$ = ± 1.3 dB, and $u_{FP}$ = ± 1 dB are standard uncertainties of spectrum analyzer and electric field probe, respectively.

Simulation results show significant deviation from the measured results. The reason lies in broadband matching balun, which was not included in the simulation model. Fig. 10a shows considerable decrease of antenna gain when the matching balun is mounted on the antenna (especially below 500 MHz and above 2.5 GHz). However, significant variations of input impedance of antenna without matching balun (Fig. 11) would provide very poor matching to 50 Ω devices. On the other hand, the manufacturer guarantees the input impedance of 50 Ω for the antenna with balun, with flatness better than ± 0.4 dB over the entire operational frequency range. Since the tested biconical dipole is declared as an antenna for broadband measurements, the constant input impedance of 50 Ω is essential to provide a good matching to other 50 Ω instruments.

The antenna factor and gain measurement and simulation results for both patch antennas are presented in Fig. 9 and 10. The good agreement between measurements inside and outside of GTEM cell can be noticed, especially at the resonant frequency. However, the simulation results are in good agreement with the measurement results only for resonant frequency. The reason lies in the fact that FEKO calculates the antenna gain as if there were no mismatch losses between antenna and coaxial cable. The actual gain is lower outside the resonance because the matching is achieved only in a narrow range around the resonant frequency.

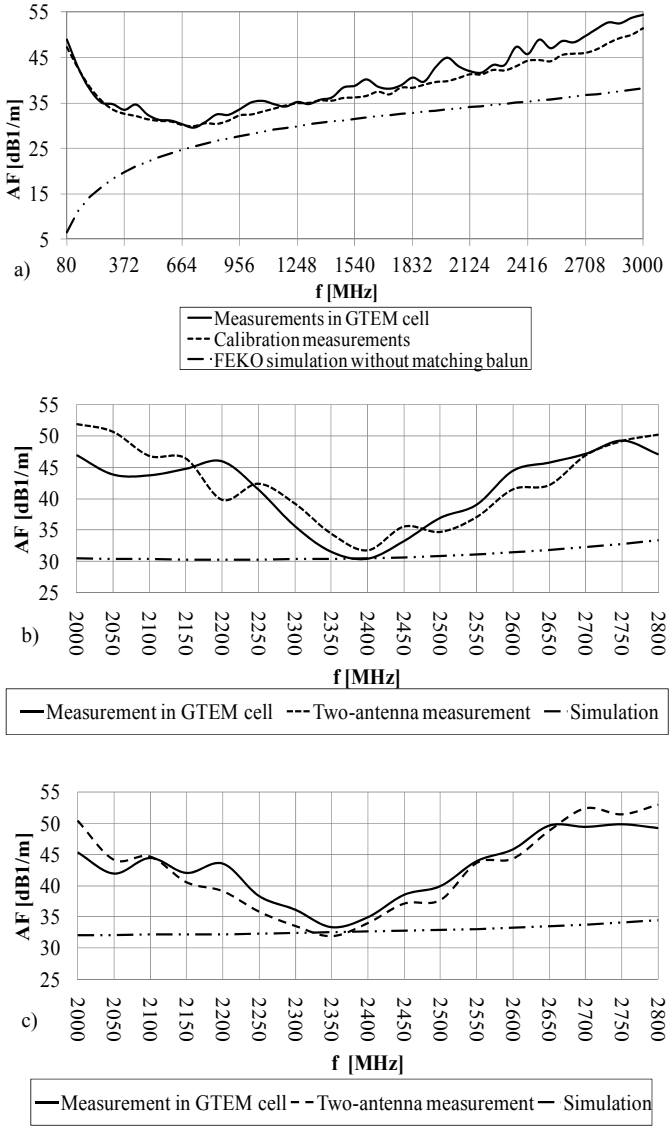


Fig. 9. Measurement and simulation results for antenna factor of a) biconical dipole, b) RMSA, c) CMSA

Table 1 summarizes the measurement, simulation and theoretical results of gain of RMSA and CMSA antennas at the resonant frequency. The theoretical results of the antenna gain were found using approximate equations given in [15] and [16].

Regarding the fact that the combined uncertainty [18] of the spectrum analyzer and the electric field probe is 1.65 dB, it is evident that the measurement results are in good agreement with those obtained by theory and simulation.

TABLE I
OVERVIEW OF MICROSTRIP ANTENNA GAINS AT THE RESONANT FREQUENCY (2.4 GHz)

| | | Measurement | | Simulation | | Theory | |
|---|---|---|---|---|---|---|---|
| | | *G* [dB] | *f* [GHz] | *G* [dB] | *f* [GHz] | *G* [dB] | *f* [GHz] |
| RMSA | In GTEM | 7.3 | 2.4 | 7.1 | 6.3 | 7.0 | 5.2 |
| | Outside GTEM | 6.1 | 2.4 | | | | |
| CMSA | In GTEM | 6.2 | 2.35 | 7.0 | 2.4 | 5.2 | 2.4 |
| | Outside GTEM | 7.6 | 2.35 | | | | |

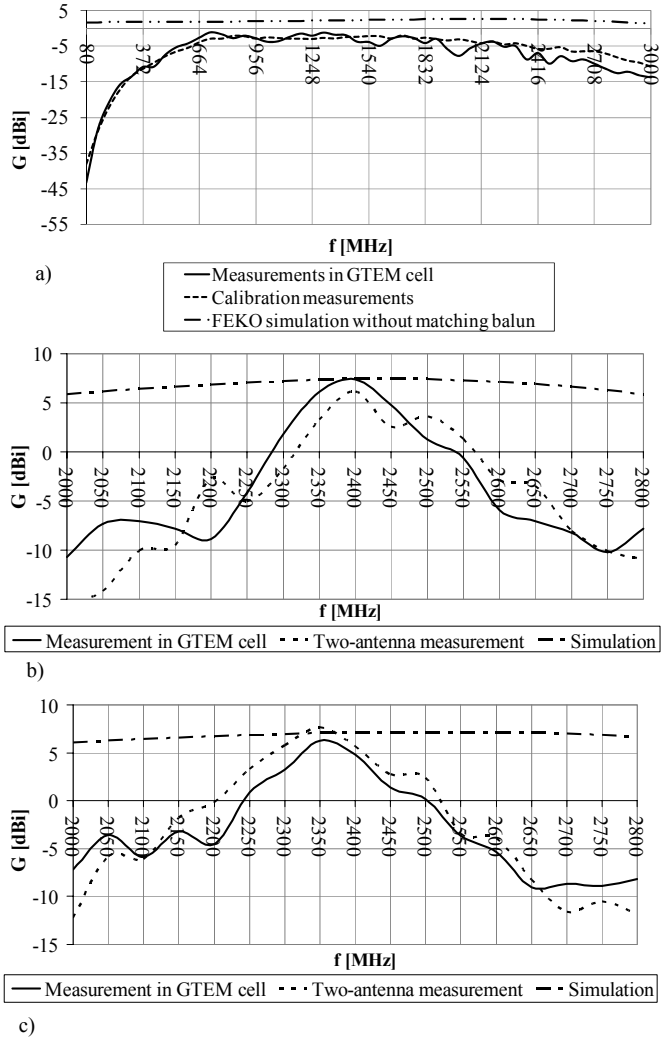


Fig. 10. Gain measurement and simulation results for: a) biconical dipole, b) RMSA, c) CMSA

*B. Results for input impedance*

Fig. 12 presents the results of impedance of the RMSA for all three measurement scenarios and the measured impedance of the CMSA antenna in GTEM cell oriented toward the absorbers. It is evident that all three different measurement scenarios yield similar results. Slight but noticeable differences could be analyzed in a separate study.

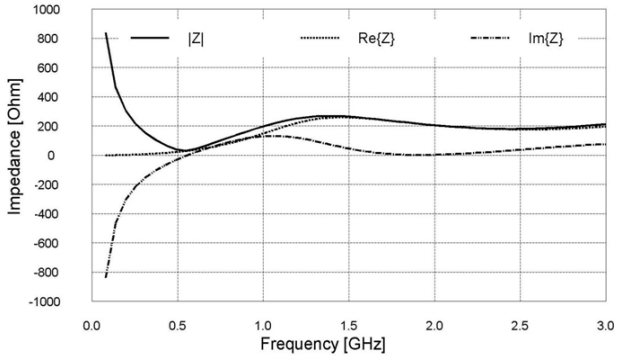


Fig. 11. Simulation results for input impedance of biconical dipole without matching balun

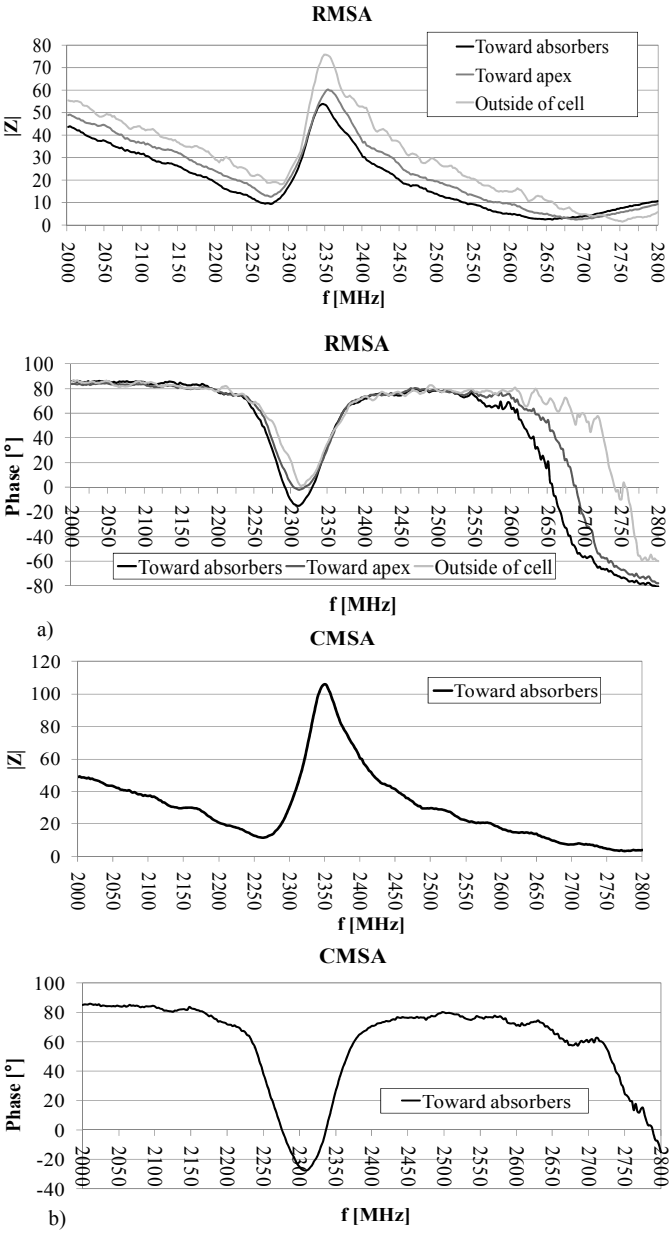


Fig. 12. Input impedance measurement results of magnitude and phase for: a) RMSA, b) CMSA

*C. Radiation pattern*

The measurement and simulation results for radiation pattern of the small loop antenna at 25.11 MHz are shown in Fig. 13. It is evident that the measured results match very well with FEKO simulation results.

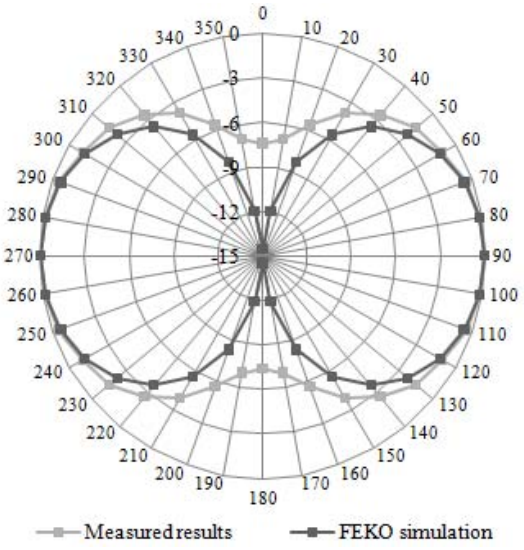


Fig. 13. Measurement and simulation results for radiation pattern of the small loop antenna

## V. CONCLUSION

In the process of antenna calibration and measurement of antenna parameters, the anechoic chambers completely covered with RF absorbers are often used. As a less expensive alternative, the GTEM cell could be used, provided that its suitability and accuracy could be verified.

In this paper the measurement setup and procedure for measuring small antenna parameters (gain, antenna factor, input impedance and radiation pattern) in the GTEM cell was proposed. As an example, a broadband biconical dipole, microstrip patch antennas, and a small loop antenna were used. However, this setup could be used for any other antenna as long as its dimensions are sufficiently small to fit into the usable test volume of the GTEM cell.

For the biconical dipole, the measurement results obtained in GTEM cell showed significant agreement with those obtained by calibration measurements which were performed in a fully absorber lined anechoic site at an accredited laboratory. These results indicate that the GTEM cell can be used as a reliable measurement environment for measurements and calibration of small antennas.

A rectangular and a circular microstrip patch antennas were designed and realized aiming for the resonant frequency of 2.4 GHz. Their gain and input impedance were measured inside a GTEM cell. The results were compared to the results obtained by free-space measurement methods performed in a low-reflective indoor environment. The obtained results show that the antennas perform well at the resonant frequency. The impedance measurements show good matching at the resonant frequency. The measured gains are in good agreement with the simulation and theory, confirming the suitability of GTEM cell.

The measurement results of radiation pattern of small loop antenna showed significant agreement with those obtained by FEKO simulation software, although the antenna dimensions were around the upper limit for the antenna dimensions that can be measured in our GTEM cell.

The methods and results presented in this paper confirm that GTEM cell is a practical and accurate environment for small antenna measurements. Its suitability for antenna measurements and calibration is comparable to that of anechoic chambers, for small antennas that fit in its test volume.

## REFERENCES

[1] *IEEE standard test procedures for antennas*, ANSI/IEEE Std. 149-1979, IEEE Press, New York, NY, 1980.

[2] *Electromagnetic compatibility (EMC) – Part 4-20: Testing and measurement techniques – Emission and immunity testing in transverse electromagnetic (TEM) waveguides*, International Standard IEC 61000-4-20, Geneva, Switzerland, 2007.

[3] A. Nothofer, D. Bozec, A. Marvin, M. Alexander, L. McCormack: *The use of GTEM cells for EMC measurements*, National Physical Laboratory, Teddington, Middlesex, United Kingdom, pp. 227-232, 2003.

[4] D. Hansen, P. Wilson, D. Koenigstein, H. Garbe: *Emission and susceptibility testing in a tapered TEM cell*, 8th International Zürich Symposium on EMC Zürich, pp. 227-232, 1989.

[5] T. Hong, C. L. Chou, A. Kuo: *Improving calibration of broadband antenna factors in a GTEM cell*, 1999 International Symposium on Electromagnetic Compatibility, Tokyo, pp. 592-595, 1999.

[6] E. Bronaugh, J. Osburn: *Measuring EMC antenna factors in the GHz transverse electromagnetic cell*, IEEE International Symposium on Electromagnetic Compatibility, Anaheim, pp. 229-231, 1992.

[7] C. Icheln, P. Vainikainen, P. Haapala: *Application of a GTEM cell to small antenna measurements*, IEEE Antennas and Propagation International Symposium, Montreal, pp. 546-549, 1997.

[8] P. Hui: *Small antenna measurements using a GTEM cell*, IEEE Antennas and Propagation International Symposium, Columbus, pp. 715-718, 2003.

[9] C. Icheln: *Methods for measuring RF radiation properties of small antennas*, PhD dissertation, Helsinki University of Technology and Radio Laboratory Publications, Espoo, 2001.

[10] *Gigahertz Transverse Electromagnetic Cell Operation Manual*, ETS Lindgren, 2008.

[11] Z. Zivkovic, A. Sarolic: *Gain and Antenna Factor Measurements of Broadband Biconical Dipole in the GTEM Cell*, 52nd International Symposium ELMAR-2010, Zadar, pp. 297-200, 2010.

[12] Z. Zivkovic, A. Sarolic: *Gain and Impedance Measurement of Microstrip Patch Antennas in GTEM Cell*, 20th International Conference on Applied Electromagnetics and Communications – ICECom 2010, Dubrovnik, pp. 1-4, 2010.

[13] D. Senic, D. Poljak, A. Sarolic: *Electromagnetic field exposure of 13.56 MHz RFID loop antenna*, 17th International Conference on Telecommunications & Computer Networks – SoftCOM 2010, Split - Bol, pp. 65-69, 2010.

[14] D. Pouhe, G. Mönich: *On the Interplay Between the Equipment Under Test and TEM Cells*, IEEE Transactions on Electromagnetic Compatibility, Vol. 50, No. 1, pp.3-12, 2008.

[15] G. Kumar, K. P. Ray: "Broadband Microstrip Antennas", Artech House, Boston – London, 2003.

[16] E. Zentner: "Antennas and radiosystems", ("Antene i radiosustavi" in Croatian), Graphis, Zagreb, 2001.
[17] *FEKO Getting Started Manual*, www.feko.info
[18] *IEEE standard for calibration of electromagnetic field sensors and probes, excluding antennas, from 9 kHz to 40 GHz*, IEEE Std. 1309-2005, IEEE Press, New York, NY, 2005.

**Zlatko Živković** received the Diploma Engineer degree in Electrical Engineering in 2007 from the Faculty of Electrical Engineering, Mechanical Engineering and Naval Architecture, University of Split, Croatia.
He is currently a research assistant and PhD student at the University of Split, Faculty of Electrical Engineering, Mechanical Engineering and Naval Architecture (FESB), Department of Electronics. His research interests are: electromagnetic measurements, bioeffects of EM fields, electromagnetic compatibility (EMC) and radiocommunications.

**Antonio Šarolić** received the Diploma Engineer, MS and PhD degrees in Electrical Engineering in 1995, 2000 and 2004 from the University of Zagreb, Croatia. He was employed at the same university from 1995 to 2005, at the Faculty of Electrical Engineering and Computing (FER), Dept. of Radiocommunications. In 2006 he joined the University of Split, FESB, Department of Electronics and is now Assistant Professor in Electrical Engineering. His areas of interest are electromagnetic measurements, bioeffects of EM fields, electromagnetic compatibility (EMC) and radiocommunications.